Journal of Medicinal Chemistry

Article

Structure-based design of either #1i or #5i specific inhibitors of human immunoproteasomes

Gerjan de Bruin, Eva M. Huber, Bo-Tao Xin, Eva J. van Rooden, Karol Al-Ayed, Kyung Bo Kim, Alexei F. Kisselev, Christoph Driessen, Mario van der Stelt, Gijsbert A. van der Marel, Michael Groll, and Herman S. Overkleeft

J. Med. Chem., **Just Accepted Manuscript** • DOI: 10.1021/jm500716s • Publication Date (Web): 09 Jul 2014

Structure-based design of either β1i or β5i specific inhibitors of human immunoproteasomes

Gerjan de Bruin[†&], Eva M. Huber[§&], Bo-Tao Xin[†], Eva J. van Rooden[†], Karol Al-Ayed[†], Kyung-Bo Kim[≠], Alexei F. Kisselev[#], Christoph Driessen[‡], Mario van der Stelt[†], Gijsbert A. van der Marel[†], Michael Groll[§], Herman S. Overkleeft[†]*

From [†]Gorlaeus Laboratories, Leiden Institute of Chemistry and Netherlands Proteomics Centre, Einsteinweg 55, 2333 CC Leiden, The Netherlands, [§]Center for Integrated Protein Science at the Department Chemie, Lehrstuhl für Biochemie, Technische Unversität München, 85748 Garching, Germany, [‡]Department of Hematology and Oncology, Kantonsspital St. Gallen, 9007 St. Gallen, Switzerland, [≠]Department of Pharmaceutical Science, College of Pharmacy, University of Kentucky, Lexington, KY 40536, USA [#]Department of Pharmacology and Toxicology and Norris Cotton Cancer Center, Geisel School of Medicine at Dartmouth, 1 Medical Centre Drive HB7936, Lebanon, New Hampshire 03756, United States of America

* To whom correspondence should be addressed

[&]Gerjan de Bruin and Eva M. Huber contributed equally to this work

KEYWORDS Immunoproteasome, Proteasome inhibitors, Epoxyketone, Vinyl Sulfone, Multiple Myeloma

ABSTRACT Mammalian genomes encode seven catalytic proteasome subunits, namely β1c, β2c, β5c (assembled into constitutive 20S proteasome core particles), β1i, β2i, β5i (incorporated into immunoproteasomes) and the thymoproteasome-specific subunit, β5t. Extensive research in the past decades has yielded numerous potent proteasome inhibitors including compounds currently used in the clinic to treat multiple myeloma and mantle cell lymphoma. Proteasome inhibitors that selectively target combinations of β1c/β1i, β2c/β2i or β5c/β5i are available, yet ligands truly selective for a single proteasome activity are scarce. In this work we report the development of cell-permeable β1i as well as β5i selective inhibitors, which outperform existing leads in terms of selectivity and/or potency. These compounds are the result of a rational design strategy using known inhibitors as starting points and introducing structural features according to the X-ray structures of the murine constitutive and immunoproteasome 20S core particles.

Introduction

Proteasomes are large, multi-catalytic complexes that partake in the degradation of cytosolic, nuclear and misfolded ER proteins in most kingdoms of life.[1] The 20S core particles (CP) in which proteolysis takes place are C2-symmetrical barrel-shaped multi-protein complexes composed of four stacked rings of seven subunits each: the two inner rings consisting of seven homologous yet distinct β-subunits (β1-β7) are flanked by two outer rings composed of the α-subunits 1-7.[2] The proteolytic activity resides within three catalytic subunits (one copy in each β-ring), namely β1c (also referred to as caspase-like, cleaving preferentially after acidic residues), β2c (trypsin-like, with a preference for basic residues) and β5c (chymotrypsin-like, preferring neutral, hydrophobic residues at the cleavage site[2-3]). Immune-competent cells express next to the constitutive proteasome (cCP) the interferon-γ-

inducible subunits β1i (LMP2), β2i (MECL-1) and β5i (LMP7).[4] Upon cytokine stimulation these subunits replace their constitutive proteasome counterparts (β1c, β2c and β5c, respectively) to form immunoproteasomes (iCPs).

The substrate preference of cCP catalytic subunits considerably overlaps with their iCP analogues, though subtle differences have been observed.[5] In particular, whereas β1c prefers acidic residues at P1 (Asp or Glu; the amino acid residue residing at the C-terminus of the scissile peptide bond), β1i is biased to hydrophobic side chains at this position.[6] This divergence of substrate preference has been connected to processing and presentation of antigenic peptides from cytosolic/nuclear sources.

Proteasome inhibitors take up a prominent position both in fundamental and applied biomedical research. Based on the structural diversity of natural CP inhibitors, numerous synthetic compounds have been developed. Most of them are peptide-based and feature an electrophile that reacts with the N-terminal nucleophilic threonine hydroxyl group of catalytic proteasome subunits to form a covalent linkage. Depending on the nature of the electrophilic trap the covalent bond is transient (aldehydes, boronic acids), semi-permanent (beta-lactones) or permanent (vinyl sulfones, epoxyketones).[7] Subunit specificity is largely governed by the nature of the peptide fragment (amino acid sequence) of a given inhibitor, though examples exist in which substitution of the electrophilic head group on an otherwise unaltered compound also impacts the proteasome inhibition profile.[8] CP inhibitors are broadly used to study the proteolytic system in more detail and to modulate physiological processes, in particular cell proliferation. The finding that proteasomes are valid therapeutic targets in various cancers led to the development of the peptide boronic acid bortezomib (Velcade)[9] as a drug for the treatment of multiple myeloma (MM) and mantle cell lymphoma. This breakthrough was recently followed by the FDA approval of the peptide epoxyketone carfilzomib (Kyprolis)[10] as a second-generation CP inhibitor for the treatment of MM. Thus, both reversible and irreversible proteasome inhibitors are relevant candidates for drug

development strategies. Currently, several proteasome inhibitors are in clinical trials, including marizomib (salinosporamide A, NPI-0052), delanzomib (CEP-18770)[11], ixazomib (MLN-9708)[12], and oprozomib (ONX-0912, PR-047)[13].

Although bortezomib and carfilzomib have been developed to primarily target the chymotrypsin-like active sites β5c and β5i, which are the most important ones for the anti-tumor effects, they also co-inhibit the subunits β1c/β1i as well as β2c/β2i at higher concentrations.[10a, 14] We have contributed to this research field by the development of potent, cell permeable ligands specific for one catalytic subunit (β1[3a], β2[3b] or β5[8a, 15]) of the cCP together with its iCP counterpart. These compounds demonstrated that cytotoxicity in MM cell lines cannot be reached by exclusive blockage of β5c/β5i, but requires co-inhibition of either β1c/β1i or β2c/β2i.[3a, b] In the present study we aimed to distinguish between cCP and iCP catalytic subunits, especially given that in various lymphomas iCPs – absent in most tissues – are the predominant proteasome species. Thus, compounds specific for one out of the six catalytic subunits from which cCPs and iCPs are assembled, are highly desirable commodities for research and clinical applications nowadays. This certainly holds true for oncological research, where identification of the ideal target/dosage combination – which catalytic active site should be inhibited, and to what extent – needs to be established. Furthermore, this also applies to the immunological question of which proteolytic center is involved in the generation of a given antigenic peptide.

For many years X-ray diffraction data from yeast proteasomes (yCP) were used to clarify the mode of action and binding specificity of CP inhibitors, including approved drugs and drug candidates.[16] Recently, structure elucidation of the murine cCP and iCP complemented the yeast structures and highlighted the differences between the cCP and iCP.[17] Perusal of the differences between the two structures and their inhibitor-bound counterparts provide insight to structural features by which β1i and β5i may be targeted independently from β1c and β5c, respectively. Specifically, β5i appears to be able to accommodate a larger amino acid side

chain at position P1 than β5c, while the opposite holds true for the P3 residue. On the other hand, the S1 pocket of β1i is more hydrophobic when compared to β1c, while the S3 pocket of β1i is more restricted in size and more polar compared to its counterpart β1c.

Here we report on the discovery of inhibitors highly specific for either β5i or β1i in the presence of all constitutive proteasome and immunoproteasome active sites. The design of our β5i specific inhibitors is based on two compounds previously developed by ONYX Pharmaceuticals, namely ONX-0914[18] (PR-957, **1**) and PR-924[18a, 19] (**2**) (Figure 1A). Using a structure-based design approach we obtained molecules with considerably improved selectivity for β5i over β5c. X-ray crystallographic analysis of the inhibitors in complex with the yCP provided important insights into the molecular basis of β5i selectivity. For the development of β1i selective inhibitors our previously reported β1c/β1i specific inhibitor NC-001[3a] (**3**) (Figure 1B) was used as a starting point. In a first optimization round its key structural element, a proline residue at P3,[20] was modified and in a second step structural features at P1 were varied.

Altogether, this strategy allowed us to identify either β5i or β1i selective compounds with high subunit selectivity and potency. All synthesized inhibitors were proven to be cell-permeable and active in mammalian cancer cell lines and hence, provide an excellent tool kit for the systematic evaluation of the distinct proteasomal active sites.

Results

Design, synthesis and evaluation of highly specific β5i inhibitors

The X-ray structure of **1** covalently bound to the murine cCP and iCP indicates that the phenyl moiety at position P1 induces a major conformational change in the S1 pocket of β5c, but only minor alterations in β5i.[17a] This difference in binding likely confers β5i selectivity to inhibitor **1** and we reasoned that substitution at P1 of phenylalanine epoxyketone for larger hydrophobic P1 residues should lead to compounds with enhanced β5i selectivity (Figure

1A). To determine the optimal P1 residue for this purpose, we synthesized epoxyketone analogues of **1** featuring an adamantyl- (**4**), biphenyl- (**5**), 2-naphthyl- (**6**), 1-naphthyl- (**7**) or cyclohexyl-alanine (**8**) in the P1 site (Table 1). The compounds were evaluated for their potencies against β5c and β5i in Raji-cell lysates (B-cell lymphoma cell line) by competitive activity based protein profiling (ABPP) of the β5-subunits using our β5c/β5i specific probe BODIPY-NC005 (Table 1 and S1, Figures S1 and S2).[21] In contrast to Muchamuel *et al.* who determined a 30-fold selectivity for β5i over β5c for **1**[18b] using an ELISA-based assay in MOLT-4 cells, we observed a nine-fold selectivity with our ABPP technique. The ABPP method was used for all the herein described compounds and allowed to unambiguously compare their activity and selectivity. Incorporation of adamantylalanine epoxyketone at P1 of the lead structure (**4**) resulted in complete loss of affinity. Interestingly, the bulky biphenyl side chain in **5** did not show increased selectivity but a two-to-three-fold enhanced potency for β5c and β5i. Furthermore, while the 2-naphthyl-side chain in **6** has both high affinity and increased selectivity for β5i, the 1-naphthyl derivative **7** is significantly less potent than compound **1**. Different orientations of the 1-naphthyl and 2-naphthyl substituents in the β5c/β5i active sites might explain this observation. The most prominent improvement in selectivity was noticed for **8**, featuring a cyclohexylalanine residue at P1. While the binding strength towards β5i remained similar, the affinity for β5c was significantly impaired compared to the lead structure ONX-0914 (**1**), hereby enhancing β5i selectivity almost five times.

For further optimization we thus chose three side chains: cyclohexyl (highest selectivity), biphenyl (highest potency) and phenyl (for comparison). We synthesized cyclohexyl (**9)** and biphenyl (**10)** analogues of the phenyl-bearing compound PR-924 (**2**) – another β5i selective inhibitor with 100-fold preference for β5i.[19b, 22] **9** turned out to be 500-fold selective for β5i over β5c yet with threefold lower potency compared to **2**. Compound **10** appeared less selective than **2**, indicating that a biphenyl substituent at P1 is not suitable for optimal β5i

selectivity. Next, hybrid compounds featuring elements from both **1** and **2** with various P1 amino acid derivatives were evaluated (**11**-**22**, Tables 1 and S1). From this focused set of compounds, several β5c/β5i inhibition and selectivity patterns emerge. First, differences in potency and selectivity between P2 residues such as 4-methyltyrosine (4MeTyr)- and tryptophan-derived epoxyketones are marginal. Second, the chirality (D/L) of the alanine in P3 can have significant influence on β5i selectivity and -potency. For example, the *N*-acylmorpholine capped compounds **8** and **11** show a similar selectivity profile, however **11** (featuring D-Ala in P3) is fivefold less active towards β5i and β5c compared to **8** (bearing L-Ala in P3). In contrast, the 3-methyl-*1H*-indene capped inhibitor **12** with L-Ala in P3 displays a significant decrease in selectivity but an increase in potency versus its D-Ala featuring analogue **13**. We conclude that L-Ala at P3 combines better with an *N*-acylmorpholine cap, whereas D-Ala at P3 requires a 3-methyl-*1H*-indene *N*-cap for optimal β5i selectivity. Compounds **9** and **13** show the highest β5i selectivity, indicating that D-Ala/3-methyl-*1H*-indene is preferred over L-Ala/*N*-acylmorpholine for β5i selectivity.

As previously reported, subunit selectivity of proteasome inhibitors can be influenced by the electrophilic trap.[8] For example, exchanging the epoxyketone warhead by a vinyl sulfone in β5-selective inhibitors improves β5-selectivity[8a]. Based on these results, we decided to compare the epoxyketones **1**, **2**, **8** and **9** with their vinyl sulfone counterparts **23**, **24**, **25** and **26** (Tables 1 and S1). All tested peptide epoxyketones outperform their peptide vinyl sulfone analogues where it comes to β5i inhibition potency. Of the peptide vinyl sulfone series only **25** is a moderately potent β5i inhibitor, however with four times higher selectivity for β5i compared to **2**.

The six most specific and potent epoxyketone compounds, namely **8**, **9**, **11**, **13**, **15** and the vinyl sulfone **25** were evaluated for selectivity over the other subunits, i.e. β1c/β1i and β2c/β2i using our ABPP technique in Raji cell lysates with β1c/β1i selective probe BODIPY-NC001 and pan-reactive probe BODIPY-epoxomicin (Figures 2 and S2, Table S1).[21a] The

obtained results disclose that **8** targets β1i and β2i with slightly more potency than **1**, while β1c is completely unaffected. Compound **2** and to a lesser extent **9** also co-inhibit β1i in the low micromolar range, whereas compounds **11, 13, 15** and **25** are highly specific for β5c/β5i and do not inhibit β1c/β1i and β2c/β2i at concentrations up to 10 μM.

Next, we tested the cellular potency and selectivity of **8**, **9**, **11**, **13**, **15** and **25** in RMPI-8226 (MM-cell line) (Figure 3, Table S2). All inhibitors proved to be cell-permeable and selectivity trends resemble those observed in Raji lysates. Compound **8** exhibits an increased selectivity for β5i over β5c compared to **1**. Notably, it also favors β1i and β2i over β5c, making it a broad-spectrum immunoproteasome inhibitor, when applied at a concentration of 1 μM. To the best of our knowledge, this is the first proteasome inhibitor able to selectively inhibit all three iCP subunits over their constitutive counterparts. Although the potency of the D-alanine containing compounds **11** and **15** towards β5i is decreased by a factor of 3-5, they are 4 times more selective for β5i than **1**. Moreover, the analogues **9, 13** and **25** are >10 times less reactive towards β5i compared to **2**. However, in case of **13** and **25** all other subunits remain fully active up to 100 μM (Figure 3, Table S2). In conclusion, compounds **9**, **13** and **25** are the most selective β5i inhibitors known to date.

X-ray structures of β5i specific inhibitors in complex with the yeast CP

The compounds **2**, **8**, **9**, **11** and **17** complexed with yCP were further analyzed by X-ray crystallography. Despite the high concentrations used for crystal soakings the D-Ala-featuring inhibitors **2**, **9**, **11** and **17** solely target subunit yβ5. In contrast, **1** (P3-L-Ala) was shown to inhibit all three active sites of the yCP[17a] and its cyclohexyl analogue **8** (L-Ala) occupies at least the subunits yβ5 and yβ2 (Figures 4A and S3C, Table S4). The P3-D-Ala residue hence confers selectivity for the chymotrypsin-like active sites, which is consistent with the ABPP results in Raji cell lysate and RPMI-8226 cell assays (Figures 2 and 3). Structural modeling by superposition with the murine substrate binding channels, which are built up of the two

neighboring subunits β1/2, β2/3 and β5/β6, respectively, provide explanations for this subunit preference (Sequence numbering according to Huber *et al.*[17a]).

The compounds **11** and **17** do not properly fit into the β1/β2 substrate binding channels due to clashes of their N-caps with Glu112 (β2i; 1.8 Å), His114/Tyr114 (β2i/c; 2.7-3.1 Å) and Asp120 (β2c; direct contact). Inhibition of the more polar caspase-like yβ1/β1c active sites is further disfavored by the hydrophobicity of the ligand. In addition, modeling **11** into the β2/3 substrate binding channel depicts that the *N*-acylmorpholine cap clashes with Met119 (β3) (distance 1.3-2.3 Å), thereby preventing its binding (Figure S3A).

Compound **2** and its derivative **9** preferentially bind to the subunits yβ5, β5c/i and β1i, a fact that is mostly due to the favorable interactions between their hydrophobic P1 sites and the respective protein S1 pockets. Compared to β5 subunits, the affinity for β1 active sites is reduced by a clash with His116. Polarity reasons and steric hindrance with Met96 (2.3 Å) further impair binding to the yβ1/β1c active sites. A clash of the 3-methyl-*1H*-indene cap with Leu115 (β3; 2.0-2.3 Å) as well as Asn22 (β2i; 2.6 Å) leads to reduced affinity also for the β2/3 substrate binding channel (Figure S3A).

In agreement with the β5-selectivity of the investigated compounds, no clashes with residues from the β5/6 substrate binding channels in cCP or iCP were identified. Inspection of the $2F_O$-F_C electron density maps, however, revealed pronounced differences in the binding mode of **1** and **8** compared to **11** and **17** as well as **2** and **9**. Compound **8** adopts a conformation, which is identical to **1**[17a]**,** whereas this does not apply to **11** and **17**, the P3-D-Ala analogues of **1** and **8** (Figures 4 and S3). The inverted chirality induces a sharp (almost 90°) turn in the peptide backbone of **11** and **17** and forces their P3 site as well as their *N*-acylmorpholine cap to undergo unique interactions. By contrast, binding of **2** and its analogue **9**, both featuring a D-Ala at P3 in combination with a 3-methyl-*1H*-indene cap is comparable to that of **1** and **8** (Figure 4). Our structure-affinity relationship studies also indicate that a cyclohexyl side chain in P1 disfavors binding to β5c and thereby enhances selectivity for β5i

compared to a phenyl group. Notably, structural superpositions of the yCP-bound compounds **1**, **2**, **8**, **9** as well as **17** reveal similar conformations of their P1 site (Figure S3B).

Development of β1i specific inhibitors

The crystal structures of the murine cCP and iCP depict differences between the substrate binding channels of β1c and β1i to exist predominantly in the S1 and S3 pockets.[17a] As a result of the substitutions T20V, T31F, R45L and T52A in β1i (relative to β1c), the cleavage preference for acidic residues at P1 is largely abolished, while processing after hydrophobic amino acids is enhanced.[3c] Furthermore, the S1 and S3 pockets appear diminished in size when compared to β1c and the S3 pocket is more polar than in β1c.

For the development of β1i specific inhibitors, we chose az-NC001[9c] (**3**), a potent β1c/β1i -specific ligand as starting point (Figure 1B). Since the β1c/β1i selectivity of **3** appears to be governed by the turn-inducing P3-proline residue, we evaluated seven analogues of **3** (**27**-**33**) in which Pro was substituted for proline isosters (Figure 5A). With the aim to increase the polarity of the P3 residue we selected hydroxyproline (Hyp) (**27**) and thioproline (Thz) (**28**). The optimal ring size was determined by comparing L-azetidine-2-carboxylic acid (Aze, 4-membered ring) (**29**) and L-pipecolic acid (Pip, 6-membered ring) (**30**). Fluorinated proline analogues **31**, **32** and **33** were included to probe the effect of altering *cis/trans* ratios around the peptide bonds.[23]

The analogues **27-33** were evaluated by ABPP for blockage of β1c and β1i in Raji lysates (Figure 5B, Table S3**)**. As anticipated, **32** (P3 = *R*-4FPro) was found to be about tenfold more potent than **31** (P3 = *S*-4FPro), however, the affinity was not increased compared to **3**. Interestingly, **33** (P3 = 4,4-F_2Pro) showed a clear preference for β1i versus β1c, without loss of potency.

To further enhance β1i selectivity the P1 side chain was modified. During the evaluation of our β5i specific inhibitors, we observed that compounds bearing a phenyl or cyclohexyl

residue at P1 inhibit β1i much stronger than β1c (Figure 2B), indicating that the S1 pocket of β1i is more apolar than that of β1c.[17a] In addition, neither β1c nor β1i is inhibited by compounds featuring a biphenyl substituent at P1 (data not shown), a finding that supports structural data showing that β1c/i have a smaller S1 pocket than β5c/i.[17a] Hence, we synthesized a series of analogues of **3** with phenyl or cyclohexylalanine in P1 and Pro or 4,4-F_2Pro in P3 (Figure 6A). Compound **34** (P1 = Phe) binds to β1i without loss of potency compared to **3**, indicating that bulky residues in P1 are tolerated by β1i (Figure 6C, Table S3). Substitution of the phenylalanine moiety for cyclohexylalanine (as in **35**) further increases the selectivity by a factor of four. Combining bulky residues in P1 with 4,4-F_2Pro in P3 resulted in the compounds **36** and **37**, of which the latter showed 250-fold selectivity for β1i over β1c. In RPMI-8226 cells as well as Raji lysate, **37** is selective for β1i and as potent as **3** (Figure 6D, Table S2). Finally, we compared **37** with the epoxyketone UK-101[24] (**38)**, the so far only β1i specific inhibitor (ML-604440[25] is the only other β1i inhibitor reported, which is equipped with the reversible boronic acid warhead) (Figure 6B, Table S2). In Raji lysate, the potency of **38** for β1i is comparable to **37**, however, it is about two-fold less specific for β1i and also targets β5c/β5i before β1c (Figure 6C). In conclusion, **37** is the most specific and cell-permeable non-reversible β1i inhibitor known to date.

Discussion

The main challenge in proteasomal drug development is the design of subunit-specific inhibitors. Although compounds for β1c/β1i, β2c/β2i and β5c/β5i, respectively, are available[3a, b, 8a, 26], compounds that target only one of the catalytic active sites are still rare and often exhibit a rather narrow window of selectivity. Here we describe the development of improved β5i inhibitors as well as a new class of β1i inhibitors, using design parameters derived from previously determined crystal structures.[2-3, 27] The co-crystallization of the β5iinhibitor ONX-0914 (**1**) with the murine cCP and iCP showed that the subunit-selectivity

of **1** is mainly caused by the P1 phenyl ring.[17a] This feature causes major structural rearrangements in the backbone and the S1 pocket of the β5c subunit, whereas β5i is able to accommodate the aromatic ring without pronounced conformational changes. Hence, we assumed that larger P1 residues would further disfavor binding to β5c and enhance potency as well as selectivity for β5i. Indeed, large residues such as biphenyl (**5**) and 2-naphtyl (**6**) in P1 yielded more potent β5i inhibitors. Yet, the 1-naphthyl derivative (**7**) resulted in a 40-fold drop in activity and the adamantyl analogue (**4)** was not active at all. Interestingly, β5i selectivity is enhanced by the 2-naphthyl (**6**; three-fold) and cyclohexyl (**8**; four-fold) P1 side chains. Notably, this is due to the reduced affinity for subunit β5c. These observations indicate that only certain bulky P1 residues improve β5i selectivity and that the difference in the S1 pockets between β5c and β5i are not in their linear depth but in their bottom. This is in agreement with the X-ray structures of the murine cCP in complex with ONX-0914 (**1**), which showed that Met45 forming the bottom of the S1 pocket is displaced upon ligand docking. From a structural point of view binding of both cyclohexyl and phenyl moieties to the S1 pocket of the yβ5 subunit is identical, yet, further analysis essentially requires crystal structures of the human cCP and iCP (in complex with the investigated compounds). Removing the aromatic system tends to increase the IC_{50} values in both the β5c and β5i active sites, indicating that the π-system might interact with the sulfur of Met45 and that the strength of this contact depends on its orientation. Inverting the chirality of the P3 residue can also significantly impact β5-affinity and selectivity. Furthermore, the yCP complex structures provide detailed explanation for the β5-selectivity of the D-Ala/3-methyl-*1H*-indene compounds.

Based on the observation that our β5i inhibitors preferentially target β1i over β1c at higher concentrations, we substituted the P1 leucine epoxyketone of the β1c/β1i specific inhibitor NC-001 for either phenylalanine or cyclohexylalanine epoxyketone. The resulting compounds were indeed more specific for subunit β1i. Since the mouse cCP and iCP crystal structures

show subtle differences between the S3 pockets of β1c and β1i, a P3 Pro analogue scan using **3** as a template was performed. This analysis revealed that the 4,4F_2-Pro (**33**) induces β1i selectivity without loss of activity. Combination of the cyclohexylalanine and the 4,4F_2-Pro ultimately led to compound **37**, which has a >300 fold binding preference for β1i over all other subunits in RPMI-8226 cells.

In keeping with the tradition of naming our compounds, we termed the six improved β5i specific inhibitors LU-005i (**8)**, LU-015i (**9)**, LU-025i (**11**), LU-035i (**13)**, LU-045i (**15**), LU-055i (**25**), and the β1i specific inhibitor LU-001i (**37**), in which LU stands for Leiden University and 'i' for immunoproteasome.

The set of improved subunit-specific and cell-permeable β5i and β1i inhibitors represent a useful tool to investigate the cytotoxic effect of subunit-specific proteasome inhibition in MM cells and disease models, for which controversial data exist.[19b, 22] Future drug design strategies might concentrate on the development of inhibitors selective for the cCP subunits β1c and β5c. Two β5c selective compounds have been reported, but their selectivities are modest (about 10-20 fold compared to β5i).[13, 19b] So far, also no compounds that discriminate between the subunits β2c and β2i are available. Our compounds **1** and **8** inhibit β2i slightly more potent than β2c and might provide a basis to develop also ligands for one of the two β2-subunits, which certainly will help to understand their biological and functional difference, a question that so far could not be addressed.

Experimental procedures

General procedures

All tested compounds are >95% pure on the basis of LC-MS and NMR. ^{1}H and ^{13}C NMR spectra were recorded on a Bruker AV-400 (400 MHz) or AV-600 (600 MHz) spectrometer. Chemical shifts are given in ppm (δ) relative to CD_3OD or $CDCl_3$ as internal standard. LC-MS analysis was performed on a Finnigan Surveyor HPLC system with a Gemini C18 50 ×

4.60 mm column (detection at 200−600 nm) coupled to a Finnigan LCQ Advantage Max mass spectrometer with ESI. The applied buffers were H_2O, MeCN and 1.0% TFA in H_2O (0.1% TFA end concentration). Methods used are: 15 min (0→0.5 min: 10% MeCN; 0.5→10.5 min: 10% → 90% MeCN; 10.5→12.5 min: 90% MeCN; 12.5→15 min: 90% → 10% MeCN) or 12.5 min (0→0.5 min: 10% MeCN; 0.5→8.5 min: 10% → 90% MeCN; 8.5→10.5 min: 90% MeCN; 10.5→12.5 min: 90% → 10% MeCN). HPLC purification was performed on a Gilson HPLC system coupled to a Phenomenex Gemini C18 5μm 250×10 mm column and a GX281 fraction collector.

General procedure for azide couplings

Compounds **4-37** were prepared via azide coupling of properly protected tripeptide hydrazide and properly deprotected vinyl sulfone amines and epoxyketone amines. The appropriate hydrazide was dissolved in 1:1 DMF:DCM (v/v) and cooled to -30 °C. tBuONO (1.1 equiv) and HCl (4M solution in 1,4-dioxane, 2.8 equiv) were added and the mixture was stirred for 3h at -30 °C after which TLC analysis (10% MeOH/DCM, v/v) showed complete consumption of the starting material. The epoxyketone or vinyl sulfone was added as a free amine to the reaction mixture as a solution in DMF. DiPEA (5 equiv) was added to the reaction mixture, and this mixture was allowed to warm to RT slowly overnight. The mixture was diluted with EtOAc and extracted with H_2O (3×). The organic layer was dried over $MgSO_4$ and purified by flash column chromatography (1-5% MeOH in DCM) and HPLC-purification (if necessary). Peptide hydrazides were prepared by hydrazinolysis of peptide methyl esters synthesized by standard procedures of solution peptide chemistry as described in Supporting Information.

MorphAc-Ala-Tyr(OMe)-Cha-EK (8). Compound **8** was obtained by the general protocol for azide coupling on a 50 μmol scale. Purification by column chromatography (2→4% MeOH in DCM) provided the title compound (21.88 mg, 74.5%) as a white powder after lyophilization. ^{1}H NMR (400 MHz, Chloroform-d) δ 7.45 (d, J = 7.5 Hz, 1H), 7.10 (d, J = 8.6

Hz, 2H), 6.85 – 6.69 (m, 3H), 6.27 (d, *J* = 7.7 Hz, 1H), 4.62 – 4.49 (m, 2H), 4.49 – 4.34 (m, 1H), 3.76 (s, 3H), 3.69 (t, *J* = 4.5 Hz, 4H), 3.25 (d, *J* = 5.0 Hz, 1H), 3.03 – 2.91 (m, 3H), 2.90 – 2.81 (m, 2H), 2.49 – 2.38 (m, 4H), 1.85 – 1.51 (m, 6H), 1.49 (s, 3H), 1.35 (d, *J* = 7.0 Hz, 3H), 1.25 – 1.06 (m, 5H), 0.88 (dd, *J* = 15.7, 7.9 Hz, 2H). ^{13}C NMR (101 MHz, $CDCl_3$) δ 208.24, 171.99, 170.71, 170.30, 158.66, 130.50, 128.35, 114.07, 67.03, 61.72, 59.15, 55.31, 54.39, 53.86, 52.51, 49.74, 48.43, 38.63, 36.81, 34.42, 34.02, 31.98, 26.42, 26.33, 26.05, 17.84, 16.83. LC-MS (linear gradient 10 → 90% MeCN, 0.1% TFA, 15 min): R_t (min): 6.62 (ESI-MS (m/z): 587.13 ($M+H^+$)). HRMS: calcd. for $C_{31}H_{46}N_4O_7$ 587.34393 $[M+H]^+$; found 587.34393.

MorphAc-D-Ala-Tyr(OMe)-Cha-EK (11) Compound **11** was obtained by the general protocol for azide coupling on a 50 μmol scale. Purification by column chromatography (1→3% MeOH in DCM) provided the title compound (23.19 mg, 79.0%) as a white powder after lyophilisation.^{1}H NMR (400 MHz, Chloroform-d) δ 7.56 (d, *J* = 6.9 Hz, 1H), 7.11 (d, *J* = 8.5 Hz, 2H), 6.81 (d, *J* = 8.5 Hz, 2H), 6.58 (d, *J* = 8.1 Hz, 1H), 6.36 (d, *J* = 7.8 Hz, 1H), 4.65 – 4.48 (m, 2H), 4.34 (t, *J* = 7.1 Hz, 1H), 3.77 (s, 3H), 3.72 (t, *J* = 4.5 Hz, 4H), 3.27 (d, *J* = 5.0 Hz, 1H), 3.10 – 2.91 (m, 4H), 2.86 (d, *J* = 5.0 Hz, 1H), 2.60 – 2.46 (m, 4H), 1.65 (td, *J* = 38.0, 37.2, 13.3 Hz, 6H), 1.48 (s, 3H), 1.31 (d, *J* = 7.0 Hz, 3H), 1.27 – 1.10 (m, 5H), 0.93 – 0.83 (m, 2H). ^{13}C NMR (101 MHz, $CDCl_3$) δ 208.29, 171.77, 170.65, 158.79, 130.54, 128.18, 114.17, 67.06, 61.76, 59.15, 55.34, 54.18, 53.89, 52.46, 49.63, 48.86, 38.48, 37.10, 34.31, 34.02, 32.00, 26.44, 26.28, 26.01, 17.87, 16.81. LC-MS (linear gradient 10 → 90% MeCN, 0.1% TFA, 15 min): R_t (min): 6.80 (ESI-MS (m/z): 587.27 ($M+H^+$)) HRMS: calcd. for $C_{31}H_{46}N_4O_7$ 587.34393 $[M+H]^+$; found 587.34393.

3MeIndAc-D-Ala-Tyr(OMe)-Cha-EK (13). Compound **13** was obtained by the general protocol for azide coupling on a 50 μmol scale. Purification by column chromatography (1→2% MeOH in DCM) provided the title compound (23.50 mg, 76.3%) as a white powder after lyophilization. ^{1}H NMR (400 MHz, Chloroform-d) δ 7.45 (t, *J* = 5.7 Hz, 2H), 7.38 –

7.29 (m, 2H), 7.12 (d, *J* = 8.5 Hz, 2H), 6.94 (d, *J* = 8.0 Hz, 1H), 6.78 (d, *J* = 8.5 Hz, 2H), 6.49 (dd, *J* = 7.4, 2.7 Hz, 2H), 4.70 – 4.47 (m, 3H), 3.70 (s, 3H), 3.58 (s, 2H), 3.24 (d, *J* = 5.0 Hz, 1H), 3.01 (ddt, *J* = 22.1, 14.4, 7.6 Hz, 2H), 2.83 (d, *J* = 5.0 Hz, 1H), 2.51 (s, 3H), 1.78 – 1.45 (m, 5H), 1.43 (s, 3H), 1.38 (d, *J* = 7.0 Hz, 3H), 1.31 – 0.94 (m, 6H), 0.91 – 0.77 (m, 2H). ^{13}C NMR (101 MHz, $CDCl_3$) δ 208.31, 172.53, 170.87, 166.10, 158.74, 148.39, 145.57, 142.22, 131.44, 130.54, 128.30, 127.48, 126.89, 123.91, 120.94, 114.09, 59.14, 55.25, 54.38, 52.47, 49.74, 49.10, 38.55, 38.32, 37.00, 34.34, 33.97, 31.99, 26.39, 26.24, 25.98, 18.49, 16.79, 12.50. LC-MS (linear gradient 10 → 90% MeCN, 0.1% TFA, 15 min): R_t (min): 10.44 (ESI-MS (m/z): 616.13 ($M+H^+$)) HRMS: calcd. for $C_{36}H_{45}N_3O_6$ 616.33811 $[M+H]^+$; found 616.33813.

MorphAc-D-Ala-Trp-Cha-EK (15). Compound **15** was obtained by the general protocol for azide coupling on a 50 μmol scale. Purification by column chromatography (1→3% MeOH in DCM) provided the title compound (23.27 mg, 78.1%) as a white powder after lyophilisation.^{1}H NMR (400 MHz, Chloroform-d) δ 8.35 (s, 1H), 7.67 (d, *J* = 7.8 Hz, 1H), 7.56 (d, *J* = 6.9 Hz, 1H), 7.36 (d, *J* = 8.1 Hz, 1H), 7.23 – 7.07 (m, 3H), 6.77 (d, *J* = 7.7 Hz, 1H), 6.28 (d, *J* = 7.7 Hz, 1H), 4.69 (q, *J* = 7.3 Hz, 1H), 4.53 – 4.43 (m, 1H), 4.36 (p, *J* = 7.1 Hz, 1H), 3.81 – 3.62 (m, 4H), 3.32 (dd, *J* = 14.6, 5.7 Hz, 1H), 3.23 – 3.07 (m, 2H), 2.95 (s, 2H), 2.82 (d, *J* = 5.0 Hz, 1H), 2.50 (tt, *J* = 11.7, 7.2 Hz, 4H), 1.73 – 1.57 (m, 4H), 1.45 (s, 5H), 1.31 (d, *J* = 7.0 Hz, 3H), 1.21 – 1.00 (m, 5H), 0.90 – 0.79 (m, 2H). ^{13}C NMR (101 MHz, $CDCl_3$) δ 208.33, 171.87, 171.00, 136.31, 127.49, 123.61, 122.40, 119.91, 118.87, 111.42, 110.35, 67.02, 61.74, 59.09, 53.85, 53.80, 52.52, 49.74, 48.85, 38.51, 34.23, 33.94, 31.99, 27.96, 26.41, 26.23, 26.01, 18.02, 16.81. LC-MS (linear gradient 10 → 90% MeCN, 0.1% TFA, 15 min): R_t (min): 6.85 (ESI-MS (m/z): 596.20 ($M+H^+$)) HRMS: calcd. for $C_{32}H_{45}N_5O_6$ 596.34426 $[M+H]^+$; found 596.34418.

3MeIndAc-D-Ala-Trp-Cha-EK (9). Compound **9** was obtained by the general protocol for azide coupling on a 50 μmol scale. Purification by column chromatography (1→2% MeOH in

DCM) provided the title compound (23.45 mg, 75%) as a white powder after lyophilization. ^{1}H NMR (400 MHz, Chloroform-d) δ 8.53 – 8.48 (m, 1H), 7.66 (d, *J* = 7.8 Hz, 1H), 7.43 (t, *J* = 7.2 Hz, 2H), 7.38 – 7.28 (m, 3H), 7.17 – 7.02 (m, 4H), 6.61 (d, *J* = 6.9 Hz, 1H), 6.53 (d, *J* = 7.7 Hz, 1H), 4.77 (q, *J* = 7.0 Hz, 1H), 4.55 – 4.45 (m, 2H), 3.54 (s, 2H), 3.29 (dd, *J* = 14.7, 6.5 Hz, 1H), 3.24 – 3.11 (m, 2H), 2.80 (d, *J* = 5.0 Hz, 1H), 2.48 (s, 3H), 1.72 – 1.38 (m, 9H), 1.33 (d, *J* = 7.0 Hz, 3H), 1.20 – 0.97 (m, 5H), 0.80 (d, *J* = 11.4 Hz, 2H). ^{13}C NMR (101 MHz, $CDCl_3$) δ 208.40, 172.66, 171.31, 166.10, 148.10, 145.58, 142.28, 136.31, 131.61, 127.48, 127.39, 126.84, 123.91, 123.74, 122.22, 120.90, 119.75, 118.79, 111.38, 110.35, 59.15, 53.85, 52.53, 49.92, 49.27, 38.33, 34.31, 33.90, 31.99, 27.80, 26.38, 26.19, 25.98, 18.46, 16.83, 12.48. LC-MS (linear gradient 10 → 90% MeCN, 0.1% TFA, 15 min): R_t (min): 10.36 (ESI-MS (m/z): 625.13 ($M+H^+$)). HRMS: calcd. for $C_{37}H_{44}N_4O_5$ 625.33845 $[M+H]^+$; found 625.33844.

3MeIndAc-Ala-Tyr(OMe)-Phe-VS (25)

Compound **25** was obtained by the general protocol for azide coupling on a 50 μmol scale. Purification by column chromatography (1→3% MeOH in DCM) provided the title compound (15.11 mg, 47.3%) as a white powder after lyophilization. Isolated with 16% *cis* isomer. Peaks reported correspond to *trans* isomer. ^{1}H NMR (400 MHz, Chloroform-d) δ 8.24 (s, 1H), 7.61 (d, *J* = 7.6 Hz, 1H), 7.45 (dd, *J* = 6.3, 2.3 Hz, 2H), 7.38 – 7.30 (m, 3H), 7.24 – 7.09 (m, 5H), 7.06 (dd, *J* = 7.3, 1.9 Hz, 2H), 6.95 (d, *J* = 8.6 Hz, 1H), 6.76 (d, *J* = 2.2 Hz, 1H), 6.68 (dd, *J* = 15.0, 4.4 Hz, 2H), 6.32 (d, *J* = 5.7 Hz, 1H), 6.15 (dd, *J* = 15.1, 1.7 Hz, 1H), 4.92 (dt, *J* = 12.1, 6.0 Hz, 1H), 4.81 – 4.68 (m, 1H), 4.23 (q, *J* = 6.7 Hz, 1H), 3.63 – 3.43 (m, 2H), 3.35 (dd, *J* = 14.6, 5.1 Hz, 1H), 3.22 – 3.09 (m, 1H), 2.76 (d, *J* = 7.6 Hz, 2H), 2.70 (s, 3H), 2.54 – 2.44 (m, 3H), 1.42 (d, *J* = 7.0 Hz, 3H). ^{13}C NMR (101 MHz, $CDCl_3$) δ 173.04, 171.06, 166.84, 148.99, 146.31, 145.34, 142.25, 136.68, 136.17, 130.83, 129.98, 129.79, 129.36, 128.75, 128.62, 127.76, 127.54, 126.99, 126.94, 124.03, 123.48, 122.50, 121.09, 119.97, 118.47, 111.70, 109.63, 54.34, 50.90, 50.30, 43.75, 42.65, 39.50, 38.36, 26.96, 17.43,

12.71. LC-MS (linear gradient 10 → 90% MeCN, 0.1% TFA, 12.5 min): R_t (min): 7.78 (ESI-MS (m/z): 639.13 ($M+H^+$)). HRMS: calcd. for $C_{36}H_{38}N_4O_5S$ 639.26357 $[M+H]^+$; found 639.26355.

N_3Gly-Ala-4,4-F_2Pro-Nle-ChaEK (37). Compound **37** was obtained by the general protocol for azide coupling on a 50 μmol scale. Purification by column chromatography (0→2% MeOH in DCM) provided the title compound (14.01 mg, 46%) as a white powder after lyophilization. Complex NMR due to a 2.5:1 ratio of rotamers. ^{1}H NMR (400 MHz, Chloroform-d, peaks of major rotamer) δ 7.08 (d, *J* = 7.3 Hz, 1H), 6.95 (d, *J* = 7.7 Hz, 1H), 6.13 (d, *J* = 7.9 Hz, 1H), 4.78 (dd, *J* = 9.3, 5.5 Hz, 1H), 4.67 (t, *J* = 7.1 Hz, 1H), 4.63 – 4.53 (m, 1H), 4.32 (td, *J* = 7.7, 5.6 Hz, 1H), 4.26 – 4.07 (m, 1H), 4.00 (d, *J* = 4.2 Hz, 2H), 3.91 – 3.79 (m, 1H), 3.28 (d, *J* = 5.0 Hz, 1H), 3.04 – 2.91 (m, 1H), 2.89 (d, *J* = 5.0 Hz, 1H), 2.65 – 2.48 (m, 1H), 1.87 – 1.54 (m, 10H), 1.51 (s, 3H), 1.39 (d, *J* = 6.9 Hz, 3H), 1.35 – 1.07 (m, 9H), 0.88 (t, *J* = 7.0 Hz, 3H). ^{13}C NMR (151 MHz, $CDCl_3$, all peaks reported) δ 209.85, 208.58, 172.22, 171.73, 171.56, 171.28, 168.78, 168.67, 168.58, 166.34, 126.18 (t, *J* = 241.6 Hz), 59.24, 59.07, 59.03, 58.91, 58.06, 56.08, 53.73, 53.57 (t, *J* = 33 Hz), 52.59, 52.54, 52.50, 52.17, 49.95, 48.70, 47.79, 46.82, 38.58, 35.62 (t, *J* = 25.7 Hz), 34.48, 34.23, 34.09, 32.21, 32.02, 31.97, 31.32, 28.05, 27.37, 26.45, 26.42, 26.31, 26.03, 22.47, 22.23, 18.08, 16.89, 16.69, 16.65, 14.03, 13.97. . LC-MS (linear gradient 10 → 90% MeCN, 0.1% TFA, 12.5 min): R_t (min): 7.91 (ESI-MS (m/z): 612.27 ($M+H^+$)). HRMS: calcd. for $C_{28}H_{43}F_2N_7O_6$ 612.33157 $[M+H]^+$; found 612.33154.

The synthesis of compound **1-3** has been described elsewhere.[3a, 18a] Synthetic procedures and analytical data for remaining compounds are provided in Supporting Information.

Biological analysis. *Materials.* Activity based probes were synthesized as described previously.[21a, 28]

Competition Assays in Cell Lysate. Lysates of Raji cells were prepared by sonication in 3 volumes of lysis buffer containing 50 mM Tris pH 7.5, 1 mM DTT, 5 mM $MgCl_2$, 250 mM sucrose, 2 mM ATP, and 0.025% digitonin. Protein concentration was determined by the Bradford assay. Cell lysates (diluted to 10-15 μg total protein in buffer containing 50 mM Tris pH 7.5, 2 mM DTT, 5 mM $MgCl_2$, 10% glycerol, 2 mM ATP) were exposed to the inhibitors for 1 h at 37 °C prior to incubation with AzidoBODIPY-MeTyr-Phe-Leu-VS (BODIPY-NC005; 0.1-0.5 μM; to probe β5), BODIPY-epoxomicin (0.5 μM; to probe all subunits, used for β2-profiling) or BODIPY-FL-Ala-Pro-Nle-Leu-EK (BODIPY-NC001; 1 μM; to probe β1 activity. This probe does bind slightly to β5i, so lysates were treated for 1 h with NC005VS[8a] (5 μM), prior to probe incubation for an additional 1 h at 37 °C, followed by 3 min boiling with a reducing gel-loading buffer and fractionation on 12.5% SDS-PAGE. In-gel detection of residual proteasome activity was performed in the wet gel slabs directly on a ChemiDoc™ MP System using Cy3 settings to detect BODIPY-NC005 and BODIPY-epoxomicin and Cy2 settings to detect BODIPY-NC001. Intensities of bands were measured by fluorescent densitometry and normalized to the intensity of bands in mock-treated extracts. Average values of at least two or three independent experiments were plotted against inhibitor concentrations. IC_{50} (inhibitor concentrations giving 50% inhibition) values were calculated using GraphPad Prism software.

Competition Assays in living RPMI-8226 cells. RPMI-8226 were cultured in RPMI-1640 media supplemented with 10% fetal calfs serum, GlutaMAX™, penicillin, streptomycin in a 5% CO_2 humidified incubator. 5-8 × 10^5 cells/mL were exposed to inhibitors for 1 h at 37 °C. Cells were harvested and washed with twice with PBS. Cell pellets were treated with lysis buffer (50 μL: 50 mM Tris pH 7.5, 2 mM DTT, 5 mM $MgCl_2$, 10% glycerol, 2 mM ATP, 0.05% digitonin) on ice for 1.5 h, followed by centrifugation at 14000 rpm for 15 min. Proteasome inhibition in the obtained cell lysates was determined using the method described above. Intensities of bands were measured by fluorescent densitometry and divided by the

intensity of bands in mock-treated extracts. Gels were stained by Coomassie Brilliant Blue, which was used to correct for gel loading differences. Average values of two or three independent experiments were plotted against inhibitor concentrations. IC_{50} (inhibitor concentrations giving 50% inhibition) values were calculated using GraphPad Prism software.

Crystallographic analysis.

yCP crystals were grown by hanging drop vapour diffusion as previously described.[29] Crystal drops were incubated for 12 h with 5 µl of cryo protectant and 0.5 µl of inhibitor (concentration: 50 mM in DMSO). Diffraction datasets were collected using synchrotron radiation of λ=1.0 Å at the beamline X06SA, Swiss Light Source (SLS), Villigen, Switzerland. Structure determination was performed as previously reported.[29] For model building the programs SYBYL, MAIN[30] and COOT[31] were used. Refinement with REFMAC5[32] yielded excellent R factors as well as r.m.s.d. bond and angle values. Coordinates were confirmed to fulfill the Ramachandran plot (Table S4). Figures were prepared with PyMOL.

ASSOCIATED CONTENT

Assays of compounds **1**-**26** in Raji lysates, pIC_{50} values and standard errors of all compounds in cell lysates and intact cells, structures of activity based probes, supplementary structural data, X-ray data table, complete synthetic details and characterization of all compounds and synthetic intermediates, NMR spectra and LC-MS traces of compounds **8**, **9**, **11**, **13**, **15**, **25**, **37**. This material is available free of charge via the Internet at http://pubs.acs.org.

ACCESSION CODES

4QLT (yCP-**2**), 4QLQ (yCP-**8**), 4QLU (yCP-**9**), 4QLS (yCP-**11**), 4QLV (yCP-**17**)

AUTHOR INFORMATION

Corresponding Author

* Phone: +31- 71-5274342; fax: +31-71-527-4307; e-mail: h.s.overkleeft@chem.leidenuniv.nl.

Author Contributions

&Gerjan de Bruin and Eva M. Huber contributed equally to this work

Funding Sources

This work was supported by the Netherlands Genomics Centre (Zenith Grant, to HSO) by the Deutsche Forschungsgemeinschaft (DFG, grant GR1861/10-1, to MG).

Notes

The authors declare no competing financial interest.

ACKNOWLEDGMENT

We thank the staff of the beamline X06SA at the Paul Scherrer Institute, Swiss Light Source, Villigen (Switzerland) for assistance during data collection. We are grateful to R. Feicht for large-scale purification of yeast 20S proteasomes.

ABBREVIATIONS

ABPP, activity based protein profiling; biphe, biphenylalanine; BODIPY, boron-dipyrromethene, (4,4-difluoro-5,7-dimethyl-4-bora-3a,4a-diaza-s-indacene); cCP, constitutive proteasome, DiPEA, N,N-diisopropylethylamine; EA, ethyl acetate; ek, epoxyketone; ER, endoplasmatic reticulum; Cha, cyclohexylalanine; HBTU, 2-(1H-benzotriazole-1-yl)-1,1,3,3-tetramethyluronium hexafluorophosphate; HCTU, 2-(6-chloro-1H-benzotriazol-1-yl)-1,1,3,3-tetramethyluronium hexafluorophosphate; iCP, immunoproteasome; MM, multiple myeloma; vs, methyl vinyl sulfone; pent, pentane; yCP, yeast proteasome.

REFERENCES

1. Hershko, A.; Ciechanover, A., The ubiquitin system. Annu. Rev. Biochem. 1998, 67, 425-79.

2. Lowe, J.; Stock, D.; Jap, B.; Zwickl, P.; Baumeister, W.; Huber, R., Crystal structure of the 20S proteasome from the archaeon T. acidophilum at 3.4 A resolution. Science 1995, 268 (5210), 533-539.

3. (a) Britton, M.; Lucas, M. M.; Downey, S. L.; Screen, M.; Pletnev, A. A.; Verdoes, M.; Tokhunts, R. A.; Amir, O.; Goddard, A. L.; Pelphrey, P. M.; Wright, D. L.; Overkleeft, H. S.; Kisselev, A. F., Selective Inhibitor of Proteasome's Caspase-like Sites Sensitizes Cells to Specific Inhibition of Chymotrypsin-like Sites. Chemistry & Biology 2009, 16 (12), 1278-1289; (b) Geurink, P. P.; van der Linden, W. A.; Mirabella, A. C.; Gallastegui, N.; de Bruin, G.; Blom, A. E. M.; Voges, M. J.; Mock, E. D.; Florea, B. I.; van der Marel, G. A.; Driessen, C.; van der Stelt, M.; Groll, M.; Overkleeft, H. S.; Kisselev, A. F., Incorporation of Non-natural Amino Acids Improves Cell Permeability and Potency of Specific Inhibitors of Proteasome Trypsin-like Sites. J Med Chem 2013; (c) Groll, M.; Ditzel, L.; Lowe, J.; Stock, D.; Bochtler, M.; Bartunik, H. D.; Huber, R., Structure of 20S proteasome from yeast at 2.4A resolution. Nature 1997, 386 (6624), 463-471.

4. Tanaka, K., Role of proteasomes modified by interferon-gamma in antigen processing. J Leukoc Biol 1994, 56 (5), 571-5.

5. Strehl, B.; Textoris-Taube, K.; Jäkel, S.; Voigt, A.; Henklein, P.; Steinhoff, U.; Kloetzel, P.-M.; Kuckelkorn, U., Antitopes Define Preferential Proteasomal Cleavage Site Usage. Journal of Biological Chemistry 2008, 283 (26), 17891-17897.

6. Orlowski, M.; Cardozo, C.; Michaud, C., Evidence for the presence of five distinct proteolytic components in the pituitary multicatalytic proteinase complex. Properties of two

components cleaving bonds on the carboxyl side of branched chain and small neutral amino acids. Biochemistry 1993, 32 (6), 1563-1572.

7. (a) Kisselev, Alexei F.; van der Linden, W. A.; Overkleeft, Herman S., Proteasome Inhibitors: An Expanding Army Attacking a Unique Target. Chemistry & Biology 2012, 19 (1), 99-115; (b) Beck, P.; Dubiella, C.; Groll, M., Covalent and non-covalent reversible proteasome inhibition. Biological chemistry 2012, 393 (10), 1101.

8. (a) Screen, M.; Britton, M.; Downey, S. L.; Verdoes, M.; Voges, M. J.; Blom, A. E. M.; Geurink, P. P.; Risseeuw, M. D. P.; Florea, B. I.; van der Linden, W. A.; Pletnev, A. A.; Overkleeft, H. S.; Kisselev, A. F., Nature of Pharmacophore Influences Active Site Specificity of Proteasome Inhibitors. Journal of Biological Chemistry 2010, 285 (51), 40125-40134; (b) Stein, M. L.; Cui, H.; Beck, P.; Dubiella, C.; Voss, C.; Krüger, A.; Schmidt, B.; Groll, M., Systematic Comparison of Peptidic Proteasome Inhibitors Highlights the α-Ketoamide Electrophile as an Auspicious Reversible Lead Motif. Angewandte Chemie International Edition 2014, 53 (6), 1679-1683.

9. (a) Adams, J.; Behnke, M.; Chen, S.; Cruickshank, A. A.; Dick, L. R.; Grenier, L.; Klunder, J. M.; Ma, Y.-T.; Plamondon, L.; Stein, R. L., Potent and selective inhibitors of the proteasome: Dipeptidyl boronic acids. Bioorganic & Medicinal Chemistry Letters 1998, 8 (4), 333-338; (b) Adams, J.; Palombella, V. J.; Sausville, E. A.; Johnson, J.; Destree, A.; Lazarus, D. D.; Maas, J.; Pien, C. S.; Prakash, S.; Elliott, P. J., Proteasome inhibitors: A novel class of potent and effective antitumor agents. Cancer Research 1999, 59 (11), 2615-2622; (c) Adams, J., The proteasome: a suitable antineoplastic target. Nat Rev Cancer 2004, 4 (5), 349-60.

10. (a) Demo, S. D.; Kirk, C. J.; Aujay, M. A.; Buchholz, T. J.; Dajee, M.; Ho, M. N.; Jiang, J.; Laidig, G. J.; Lewis, E. R.; Parlati, F.; Shenk, K. D.; Smyth, M. S.; Sun, C. M.; Vallone, M. K.; Woo, T. M.; Molineaux, C. J.; Bennett, M. K., Antitumor Activity of PR-171,

a Novel Irreversible Inhibitor of the Proteasome. Cancer Research 2007, 67 (13), 6383-6391; (b) Elofsson, M.; Splittgerber, U.; Myung, J.; Mohan, R.; Crews, C. M., Towards subunit-specific proteasome inhibitors: synthesis and evaluation of peptide α', β'-epoxyketones. Chemistry & Biology 1999, 6 (11), 811-822; (c) O'Connor, O. A.; Stewart, A. K.; Vallone, M.; Molineaux, C. J.; Kunkel, L. A.; Gerecitano, J. F.; Orlowski, R. Z., A Phase 1 Dose Escalation Study of the Safety and Pharmacokinetics of the Novel Proteasome Inhibitor Carfilzomib (PR-171) in Patients with Hematologic Malignancies. Clinical Cancer Research 2009, 15 (22), 7085-7091.

11. Dorsey, B. D.; Iqbal, M.; Chatterjee, S.; Menta, E.; Bernardini, R.; Bernareggi, A.; Cassarà, P. G.; D'Arasmo, G.; Ferretti, E.; De Munari, S.; Oliva, A.; Pezzoni, G.; Allievi, C.; Strepponi, I.; Ruggeri, B.; Ator, M. A.; Williams, M.; Mallamo, J. P., Discovery of a Potent, Selective, and Orally Active Proteasome Inhibitor for the Treatment of Cancer. J Med Chem 2008, 51 (4), 1068-1072.

12. Kupperman, E.; Lee, E. C.; Cao, Y.; Bannerman, B.; Fitzgerald, M.; Berger, A.; Yu, J.; Yang, Y.; Hales, P.; Bruzzese, F.; Liu, J.; Blank, J.; Garcia, K.; Tsu, C.; Dick, L.; Fleming, P.; Yu, L.; Manfredi, M.; Rolfe, M.; Bolen, J., Evaluation of the Proteasome Inhibitor MLN9708 in Preclinical Models of Human Cancer. Cancer Research 2010, 70 (5), 1970-1980.

13. Zhou, H.-J.; Aujay, M. A.; Bennett, M. K.; Dajee, M.; Demo, S. D.; Fang, Y.; Ho, M. N.; Jiang, J.; Kirk, C. J.; Laidig, G. J.; Lewis, E. R.; Lu, Y.; Muchamuel, T.; Parlati, F.; Ring, E.; Shenk, K. D.; Shields, J.; Shwonek, P. J.; Stanton, T.; Sun, C. M.; Sylvain, C.; Woo, T. M.; Yang, J., Design and Synthesis of an Orally Bioavailable and Selective Peptide Epoxyketone Proteasome Inhibitor (PR-047). J Med Chem 2009, 52 (9), 3028-3038.

14. (a) Kuhn, D. J.; Chen, Q.; Voorhees, P. M.; Strader, J. S.; Shenk, K. D.; Sun, C. M.; Demo, S. D.; Bennett, M. K.; van Leeuwen, F. W. B.; Chanan-Khan, A. A.; Orlowski, R. Z., Potent activity of carfilzomib, a novel, irreversible inhibitor of the ubiquitin-proteasome pathway, against preclinical models of multiple myeloma. Blood 2007, 110 (9), 3281-3290; (b) Kisselev, A. F.; Callard, A.; Goldberg, A. L., Importance of the Different Proteolytic Sites of the Proteasome and the Efficacy of Inhibitors Varies with the Protein Substrate. Journal of Biological Chemistry 2006, 281 (13), 8582-8590.

15. Geurink, P. P.; Liu, N.; Spaans, M. P.; Downey, S. L.; van den Nieuwendijk, A. M. C. H.; van der Marel, G. A.; Kisselev, A. F.; Florea, B. I.; Overkleeft, H. S., Incorporation of Fluorinated Phenylalanine Generates Highly Specific Inhibitor of Proteasome's Chymotrypsin-like Sites. J Med Chem 2010, 53 (5), 2319-2323.

16. (a) Borissenko, L.; Groll, M., 20S Proteasome and Its Inhibitors: Crystallographic Knowledge for Drug Development. Chemical Reviews 2007, 107 (3), 687-717; (b) Groll, M.; Kim, K. B.; Kairies, N.; Huber, R.; Crews, C. M., Crystal Structure of Epoxomicin:20S Proteasome Reveals a Molecular Basis for Selectivity of α',β'-Epoxyketone Proteasome Inhibitors. Journal of the American Chemical Society 2000, 122 (6), 1237-1238; (c) Groll, M.; Huber, R.; Potts, B. C. M., Crystal Structures of Salinosporamide A (NPI-0052) and B (NPI-0047) in Complex with the 20S Proteasome Reveal Important Consequences of β-Lactone Ring Opening and a Mechanism for Irreversible Binding. Journal of the American Chemical Society 2006, 128 (15), 5136-5141.

17. (a) Huber, Eva M.; Basler, M.; Schwab, R.; Heinemeyer, W.; Kirk, Christopher J.; Groettrup, M.; Groll, M., Immuno- and Constitutive Proteasome Crystal Structures Reveal Differences in Substrate and Inhibitor Specificity. Cell 2012, 148 (4), 727-738; (b) Huber, E. M.; Groll, M., Inhibitors for the Immuno- and Constitutive Proteasome: Current and Future

Trends in Drug Development. Angewandte Chemie International Edition 2012, 51 (35), 8708-8720.

18. (a) Shenk, K. D. P., F.; Zhou, H.-j.; Sylvain, C.; Smyth, M.S.; Bennet, M.K.; Laidig, G.J., , US/20070293465, 2007; (b) Muchamuel, T.; Basler, M.; Aujay, M. A.; Suzuki, E.; Kalim, K. W.; Lauer, C.; Sylvain, C.; Ring, E. R.; Shields, J.; Jiang, J.; Shwonek, P.; Parlati, F.; Demo, S. D.; Bennett, M. K.; Kirk, C. J.; Groettrup, M., A selective inhibitor of the immunoproteasome subunit LMP7 blocks cytokine production and attenuates progression of experimental arthritis. Nat Med 2009, 15 (7), 781-787.

19. (a) Kuhn, D. J.; Hunsucker, S. A.; Chen, Q.; Voorhees, P. M.; Orlowski, M.; Orlowski, R. Z., Targeted inhibition of the immunoproteasome is a potent strategy against models of multiple myeloma that overcomes resistance to conventional drugs and nonspecific proteasome inhibitors. Blood 2009, 113 (19), 4667-4676; (b) Parlati, F.; Lee, S. J.; Aujay, M.; Suzuki, E.; Levitsky, K.; Lorens, J. B.; Micklem, D. R.; Ruurs, P.; Sylvain, C.; Lu, Y.; Shenk, K. D.; Bennett, M. K., Carfilzomib can induce tumor cell death through selective inhibition of the chymotrypsin-like activity of the proteasome. Blood 2009, 114 (16), 3439-3447.

20. Myung, J.; Kim, K. B.; Lindsten, K.; Dantuma, N. P.; Crews, C. M., Lack of Proteasome Active Site Allostery as Revealed by Subunit-Specific Inhibitors. Mol Cell 2001, 7 (2), 411-420.

21. (a) Verdoes, M.; Willems, L. I.; van der Linden, W. A.; Duivenvoorden, B. A.; van der Marel, G. A.; Florea, B. I.; Kisselev, A. F.; Overkleeft, H. S., A panel of subunit-selective activity-based proteasome probes. Organic & Biomolecular Chemistry 2010, 8 (12), 2719-2727; (b) Li, N.; Kuo, C.-L.; Paniagua, G.; van den Elst, H.; Verdoes, M.; Willems, L. I.; van der Linden, W. A.; Ruben, M.; van Genderen, E.; Gubbens, J.; van Wezel, G. P.; Overkleeft,

H. S.; Florea, B. I., Relative quantification of proteasome activity by activity-based protein profiling and LC-MS/MS. Nat. Protocols 2013, 8 (6), 1155-1168.

22. Singh, A. V.; Bandi, M.; Aujay, M. A.; Kirk, C. J.; Hark, D. E.; Raje, N.; Chauhan, D.; Anderson, K. C., PR-924, a selective inhibitor of the immunoproteasome subunit LMP-7, blocks multiple myeloma cell growth both in vitro and in vivo. British Journal of Haematology 2011, 152 (2), 155-163.

23. (a) Renner, C.; Alefelder, S.; Bae, J. H.; Budisa, N.; Huber, R.; Moroder, L., Fluoroprolines as Tools for Protein Design and Engineering. Angewandte Chemie International Edition 2001, 40 (5), 923-925; (b) Staas, D. D.; Savage, K. L.; Sherman, V. L.; Shimp, H. L.; Lyle, T. A.; Tran, L. O.; Wiscount, C. M.; McMasters, D. R.; Sanderson, P. E. J.; Williams, P. D.; Lucas Jr, B. J.; Krueger, J. A.; Dale Lewis, S.; White, R. B.; Yu, S.; Wong, B. K.; Kochansky, C. J.; Reza Anari, M.; Yan, Y.; Vacca, J. P., Discovery of potent, selective 4-fluoroproline-based thrombin inhibitors with improved metabolic stability. Bioorganic & Medicinal Chemistry 2006, 14 (20), 6900-6916.

24. (a) Ho, Y. K.; Bargagna-Mohan, P.; Wehenkel, M.; Mohan, R.; Kim, K.-B., LMP2-Specific Inhibitors: Chemical Genetic Tools for Proteasome Biology. Chemistry & Biology 2007, 14 (4), 419-430; (b) Wehenkel, M.; Ban, J. O.; Ho, Y. K.; Carmony, K. C.; Hong, J. T.; Kim, K. B., A selective inhibitor of the immunoproteasome subunit LMP2 induces apoptosis in PC-3 cells and suppresses tumour growth in nude mice. Br J Cancer 2012, 107 (1), 53-62.

25. Basler, M.; Lauer, C.; Moebius, J.; Weber, R.; Przybylski, M.; Kisselev, A. F.; Tsu, C.; Groettrup, M., Why the Structure but Not the Activity of the Immunoproteasome Subunit Low Molecular Mass Polypeptide 2 Rescues Antigen Presentation. The Journal of Immunology 2012, 189 (4), 1868-1877.

26. Mirabella, Anne C.; Pletnev, Alexandre A.; Downey, Sondra L.; Florea, Bogdan I.; Shabaneh, Tamer B.; Britton, M.; Verdoes, M.; Filippov, Dmitri V.; Overkleeft, Herman S.; Kisselev, Alexei F., Specific Cell-Permeable Inhibitor of Proteasome Trypsin-like Sites Selectively Sensitizes Myeloma Cells to Bortezomib and Carfilzomib. Chemistry & Biology 2011, 18 (5), 608-618.

27. Unno, M.; Mizushima, T.; Morimoto, Y.; Tomisugi, Y.; Tanaka, K.; Yasuoka, N.; Tsukihara, T., Structure determination of the constitutive 20S proteasome from bovine liver at 2.75 A resolution. J Biochem 2002, 131 (2), 171-3.

28. Florea, B. I.; Verdoes, M.; Li, N.; van der Linden, W. A.; Geurink, P. P.; van den Elst, H.; Hofmann, T.; de Ru, A.; van Veelen, P. A.; Tanaka, K.; Sasaki, K.; Murata, S.; den Dulk, H.; Brouwer, J.; Ossendorp, F. A.; Kisselev, A. F.; Overkleeft, H. S., Activity-Based Profiling Reveals Reactivity of the Murine Thymoproteasome-Specific Subunit β5t. Chemistry & biology 2010, 17 (8), 795-801.

29. Groll, M.; Huber, R., Purification, Crystallization, and X-Ray Analysis of the Yeast 20S Proteasome. In Methods in Enzymology, Raymond, J. D., Ed. Academic Press: 2005; Vol. Volume 398, pp 329-336.

30. Turk, D., Improvement of a Programme for Molecular Graphics and Manipulation of Electron Densities and Its Application for Protein Structure Determination. PhD thesis, Technische Univ. München 1992.

31. Emsley, P.; Lohkamp, B.; Scott, W. G.; Cowtan, K., Features and development of Coot. Acta crystallographica. Section D, Biological crystallography 2010, 66 (Pt 4), 486-501.

32. Vagin, A. A.; Steiner, R. A.; Lebedev, A. A.; Potterton, L.; McNicholas, S.; Long, F.; Murshudov, G. N., REFMAC5 dictionary: organization of prior chemical knowledge and guidelines for its use. Acta Crystallographica Section D 2004, 60 (12-1), 2184-2195.

Table 1. Optimization of β5i selective inhibitors based on **1** (ONX-0914) and **2** (PR-924). [a,b]

[a] IC_{50} values determined using ABPP in Raji cell lysates. [b] >[conc], less than 50% inhibition at indicated concentration

Figure 1. Design principles for immunoproteasome-specific inhibitors. (A) Compounds with large hydrophobic P1 side chains display β5i selectivity. (B) Proline analogues in P3 and bulky hydrophobic P1 residues are the prerequisites to design β1i selective inhibitors.

Figure 2. (A) Chemical structures of β5i inhibitors (**8**, **9**, **11**, **13**, **15**, **25**) which show the largest improvement compared to **1** and **2**. (B) Apparent IC_{50} values of compounds in Raji cell lysates determined by ABPP.

Figure 3. Inhibition profile of selected β5i inhibitors in RPMI-8226. Cells were treated with the distinct compounds at indicated concentrations for 1 h, lysed and the occupancy of the remaining active sites was probed with BODIPY-NC005 (β5), BODIPY-epoxomicin (pan-reactive, used for β2) or BODIPY-NC001 (β1). For chemical structures see Figure S2.

Figure 4. Crystallographic analysis of yCP:ligand complexes. (A) Illustration of the yeast yβ5/6 substrate binding channel in complex with the indicated compounds. All inhibitors are covalently bound to Thr1 (black) of subunit yβ5 (yellow) by forming a morpholine ring system. Depending on the compound, the P3 site and the N-cap (marked in green) adopt different conformations. The $2F_O$-F_C electron density map for the ligand (blue) is contoured at 1 σ. The inhibitor and Thr1 have been omitted prior to phasing. (B) Structural superpositions of the ligands visualize that compounds with identical chirality and N-cap well match in their binding mode. Inversion of the P3-chirality results in a flip of the N-acylmorpholine cap. While N-acylmorpholine capped compounds adopt a bended conformation, 3-methyl-*1H*-indene N-capped inhibitors bind in an extended form due to their restricted flexibility.

Figure 5. Inhibition profiles of P3 proline analogues of 3 in Raji lysates. (A) Chemical structures of compounds **27-33**. (B) After incubation of compounds with Raji lysates for 1h, β5 activity was blocked by NC005VS for an additional hour. Subsequently, the remaining β1 activity was probed by BOPIPY-NC001.

Figure 6. **Optimization of β1i selective inhibitors.** (A) Chemical structures of compounds **34-37.** (B) Chemical structure of **38** (UK101). (C) Raji lysates were incubated with the compounds for 1h, followed by cell lysis. Lysates were probed with BODIPY-NC005 (β5), BODIPY-NC001 (β1) or BODIPY-epoxomicin (pan-reactive, used for β2) (D) Assay of the most selective β1i inhibitor **37**, compared to **3** in RPMI-8226-cells.

TOC graphic

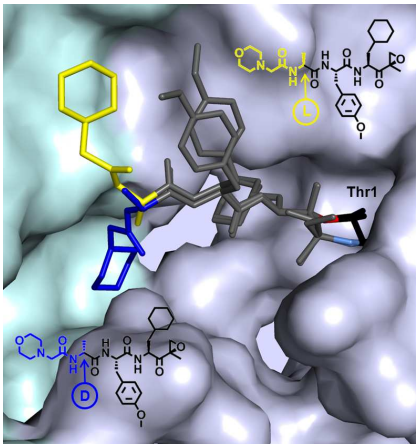

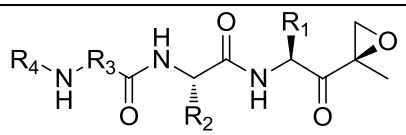					Apparent IC_{50} (nM)		Ratio
Compound	**R_4**	**R_3**	**R_2**	**R_1**	**β5i**	**β5c**	**β5c/ β5i**
1, ONX-0914	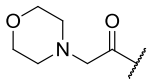		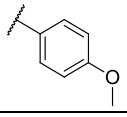		5.7	54	9
4	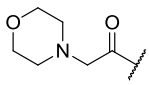		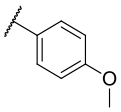	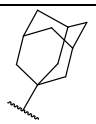	>50x10^3	>50x10^3	-
5	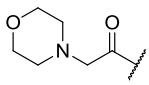		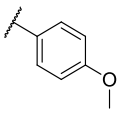	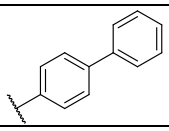	2.0	20	10
6	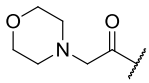		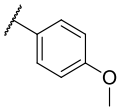	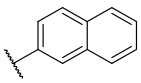	3.1	97	32
7	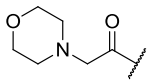		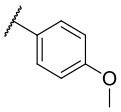	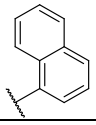	244	1.8 x 10^3	7
8, LU-005i	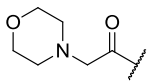		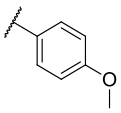		6.6	287	43
2, PR-924	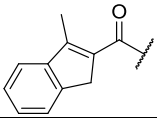		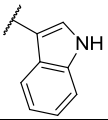		2.5	227	91
9, LU-015i	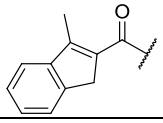		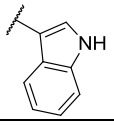		8.3	4.6x10^3	553
10	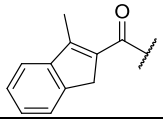		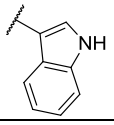	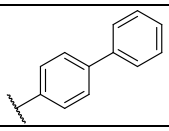	5.0	79	16
11, LU-025i	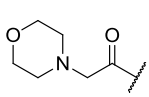		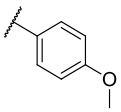		36	1.9 x 10^3	52
12					3.0	14.5	5
13, LU-035i					11	5.5 x 10^3	500

14	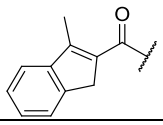		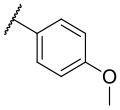		5.0	6.0	1
15, LU-045i	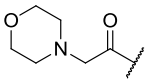		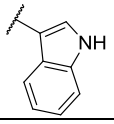		32	827	26
16	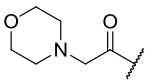		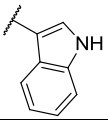		13	104	8
17	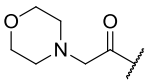		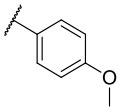		14	116	8
18	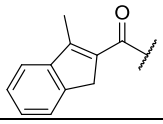		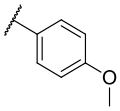		3	157	52
19	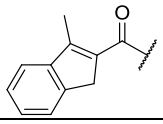		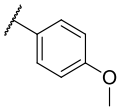	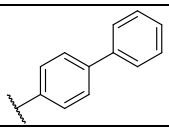	1.4	12.6	9
20	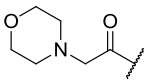		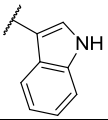	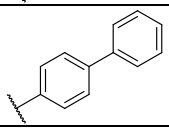	2.1	14	6
21	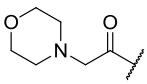		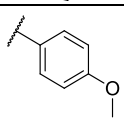	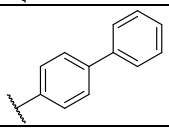	1.2	9.9	8
22	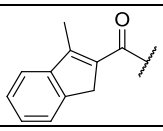		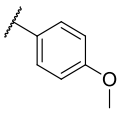	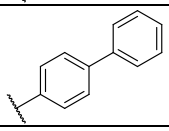	3.3	43	13
23 Vinyl Sulfone	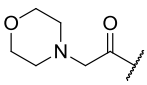		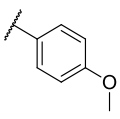		392	14×10^3	37
24 Vinyl Sulfone					5700	$>100 \times 10^3$	>18
25, LU-055i Vinyl Sulfone					53	25×10^3	464
26 Vinyl Sulfone					632	62×10^3	98

A. Towards β5i selective inhibitors

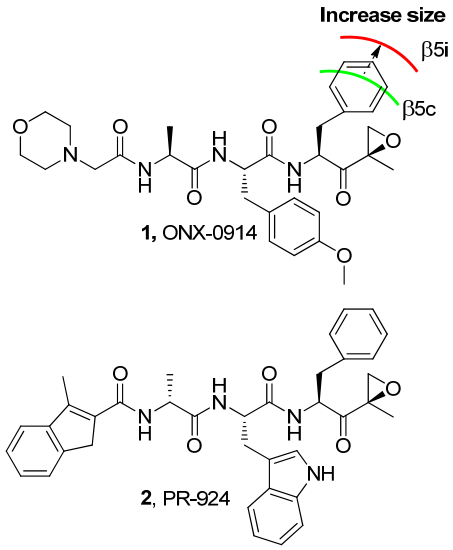

B. Towards β1i selective inhibitors

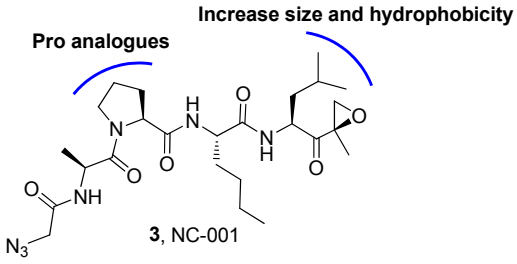

A

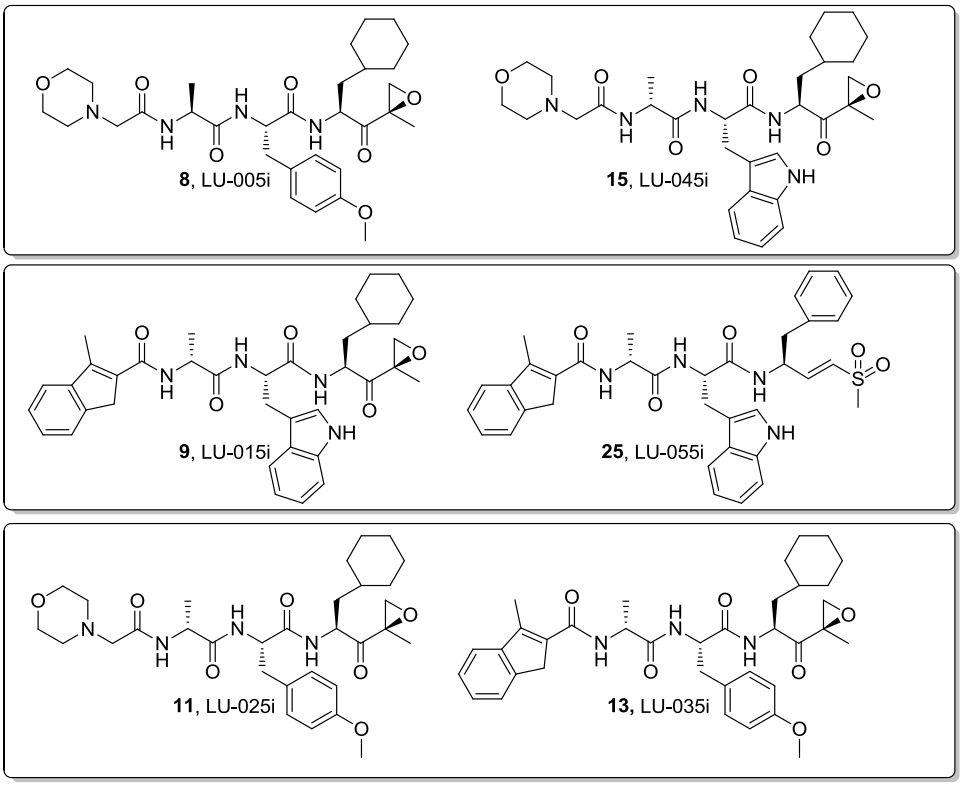

B

Compound	Apparent IC_{50} (μM) β5i	β5c	β1i	β1c	β2i	β2c	Ratio IC_{50} β5c/β5i	β1i/β5i	β2i/β5i	β2c/β5i
1, ONX-0914	0.0057	0.054	0.46	>10	0.59	1.1	9	81	103	192
8	0.0066	0.29	0.30	>10	0.41	2.5	44	45	62	378
11	0.036	1.9	>10	>10	>10	>10	52	>280	>280	>280
15	0.032	0.83	>10	>10	>10	>10	26	>312	>312	>312
2, PR-924	0.0025	0.23	1.84	>10	>10	>10	92	740	>4000	>4000
9	0.0083	4.6	7.1	>10	>10	>10	554	855	>1200	`>1200
13	0.011	5.5	>10	>10	>10	>10	500	>900	>900	>900
25	0.053	25	>100	>100	>100	>100	471	>1900	>1900	>1900

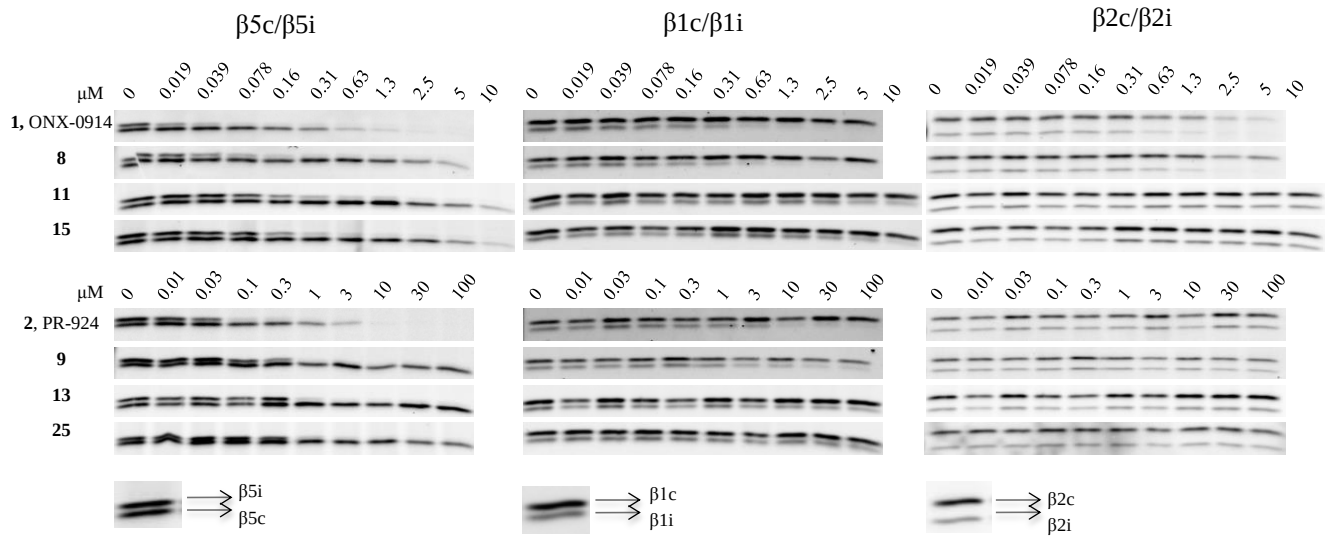

	Apparent IC_{50} (μM)						Ratio IC_{50}			
	β5i	**β5c**	**β1i**	**β1c**	**β2i**	**β2c**	**β5c/β5i**	**β1i/β5i**	**β2i/β5i**	**β2c/β5i**
1, ONX-0914	0.018	0.18	0.34	>5	0.59	1.1	10	19	33	61
8	0.044	4.2	0.37	>5	0.90	4.9	95	8	20	111
11	0.10	4.3	7.3	>10	>10	>10	43	73	>100	>100
15	0.059	2.9	6.2	>10	>10	>10	49	105	>169	>169
2, PR-924	0.025	2.9	3.5	>100	>100	>100	116	140	>400	>400
9	0.23	>100	16	>100	>100	>100	435	70	>435	>435
13	0.37	>100	>100	>100	>100	>100	>270	>270	>270	>270
25	0.39	>100	>100	>100	>100	>100	>256	>256	>256	>256

A

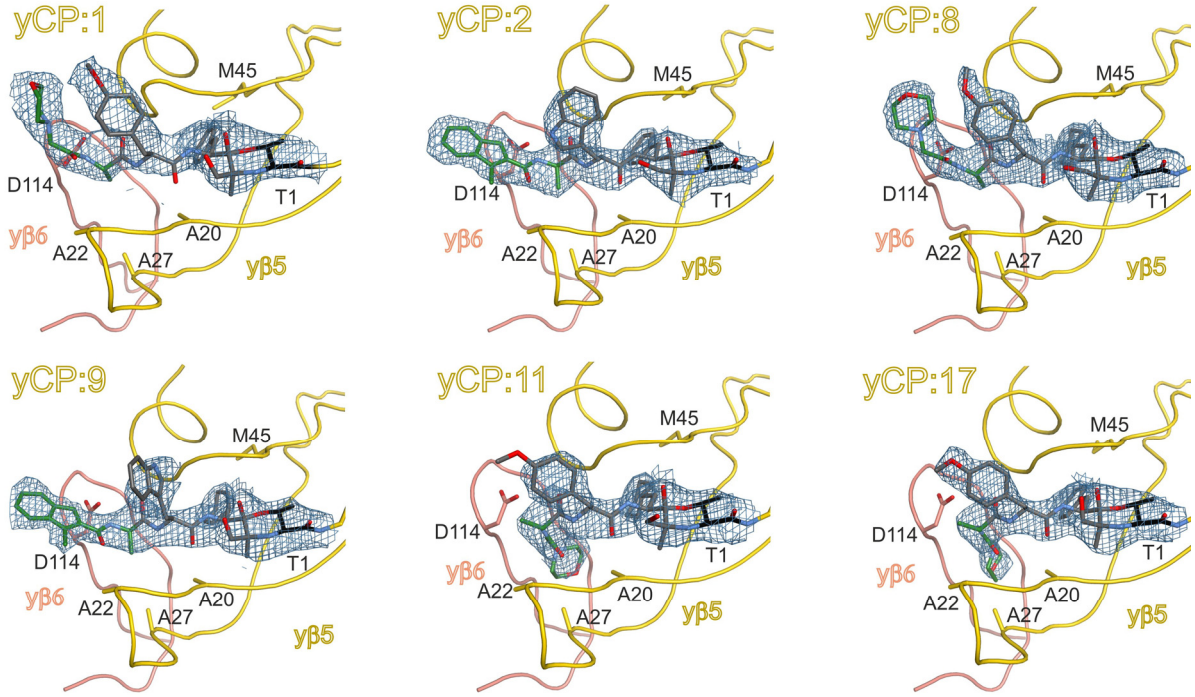
yCP:1
M45
D114
T1
yβ6
A22
A20
A27
yβ5
yCP:2
M45
D114
T1
yβ6
A22
A20
A27
yβ5
yCP:8
M45
D114
T1
yβ6
A22
A20
A27
yβ5
yCP:9
M45
D114
T1
yβ6
A22
A20
A27
yβ5
yCP:11
M45
D114
T1
yβ6
A22
A20
A27
yβ5
yCP:17
M45
D114
T1
yβ6
A22
A20
A27
yβ5

B

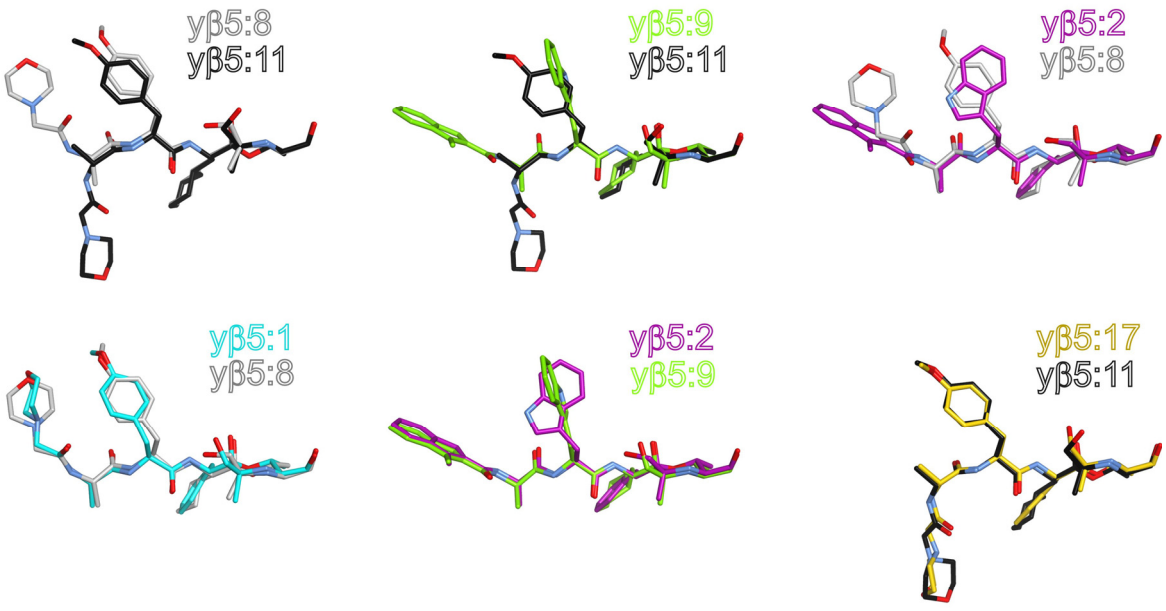
yβ5:8
yβ5:11
yβ5:9
yβ5:11
yβ5:2
yβ5:8
yβ5:1
yβ5:8
yβ5:2
yβ5:9
yβ5:17
yβ5:11

A

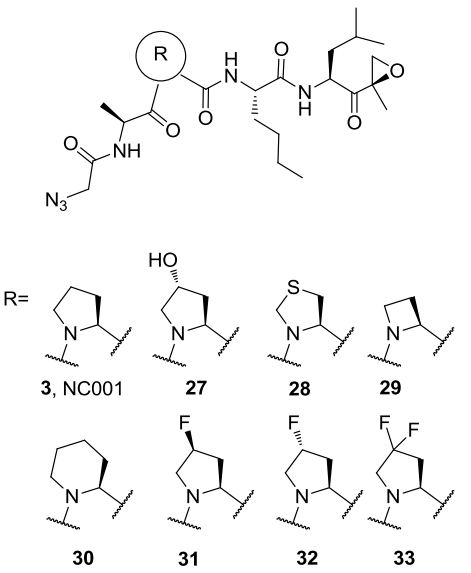

B

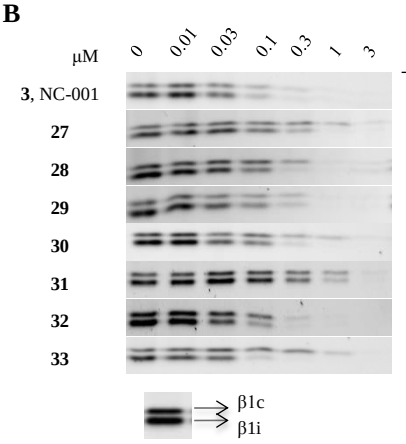

	Apparent IC_{50} (μM)		Ratio
	β1c	**β1i**	**β1c/β1i**
3, NC-001	0.088	0.045	2
27	0.86	0.17	5
28	0.24	0.068	6.5
29	0.054	0.096	0.6
30	0.25	0.067	3.7
31	0.51	0.22	2.3
32	0.066	0.022	3
33	0.36	0.034	10.5

A

Compound	R	R1
34	H	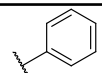
35	H	
36	F	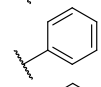
37 (LU-001i)	F	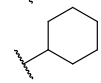

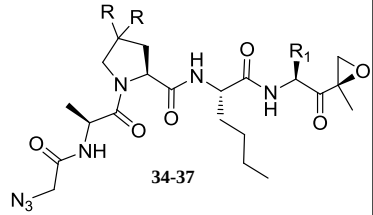

34-37

B

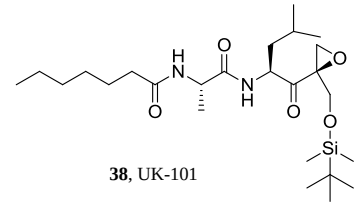

38, UK-101

C

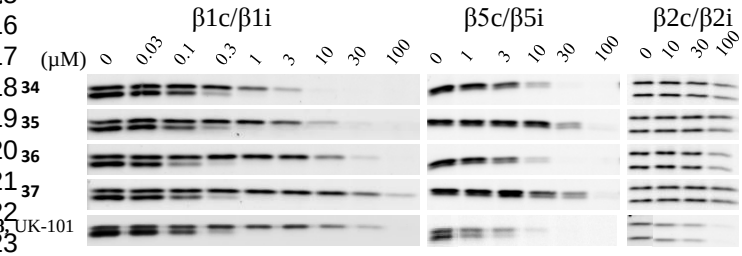

	Apparent IC_{50} (μM)				Ratio IC_{50}	
	β1i	**β1c**	**β5(i)**	**β2(i)**	**β1c/β1i**	**β1i/β5(i)**
34	0.066	0.58	4.1	>100	9	62
35	0.087	3.4	29	>30	39	333
36	0.042	4.8	3.0	>100	114	71
37	0.095	24	20	>100	252	210
38	0.104	15	1.0 (3.1)	25 (17)	144	10 (30)

D

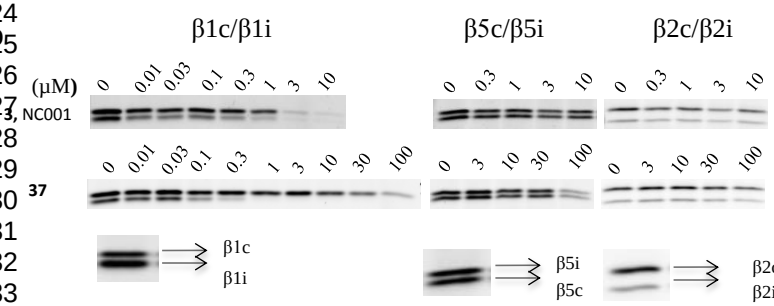

	Apparent IC_{50} (μM)				Ratio IC_{50}	
	β1i	β1c	β5c/i	β2c/i	β1c/β1i	β1i/β5c/i
3	0.14	0.37	>10	>10	3	>70
37	0.13	47	65	>100	360	500

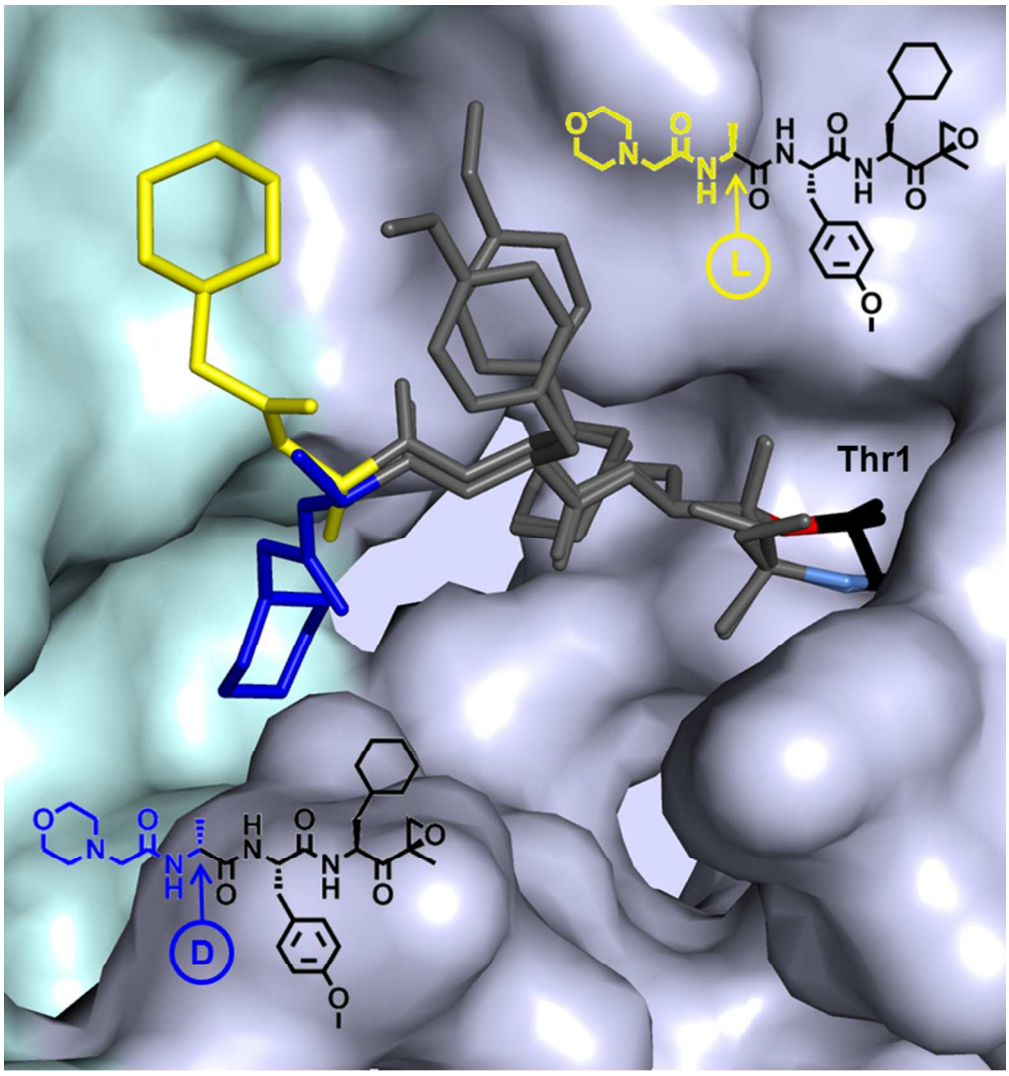

133x141mm (150 x 150 DPI)